

Effect of initial state nucleon shadowing on the elliptic flow of thermal photons

Pingal Dasgupta,^{1,2,*} Rupa Chatterjee,^{1,2,†} Sushant K. Singh,^{1,2,‡} and Jan-e Alam^{1,2,§}

¹Variable Energy Cyclotron Centre, 1/AF, Bidhan Nagar, Kolkata-700064, India

²Homi Bhabha National Institute, Training School Complex, Anushakti Nagar, Mumbai 400085, India

Recently the effect of nucleon shadowing on the Monte-Carlo Glauber initial condition was studied and its role on the centrality dependence of elliptic flow (v_2) and fluctuations in initial eccentricity for different colliding nuclei were explored. It was found that the results with shadowing effects are closer to the QCD based dynamical model as well as to the experimental data. Inspired by this outcome, in this work we study the transverse momentum (p_T) spectra and elliptic flow (v_2) of thermal photons for Au+Au collisions at RHIC and Pb+Pb collisions at the LHC by incorporating the shadowing effect to deduce the initial energy density profile required to solve the relativistic hydrodynamical equations. We find that the thermal photon spectra remain almost unaltered, however, the elliptic flow of photon is found to get enhanced significantly due to shadowing effects. We discuss the implications of these results on the initial condition and the mis-match between experimental and theoretical results on v_2 of photons.

I. INTRODUCTION

The primary goal of heavy ion collision programmes at Relativistic Heavy Ion Collider (RHIC) and Large Hadron Collider (LHC) is to produce a new state of thermalized matter called quark gluon plasma (QGP) - where the properties of the system are not governed by hadrons but by the quarks and gluons. Collisions of nuclei will create charged particles - either in the form of hadrons or partons depending on the magnitude of the collision energy. Electromagnetic interaction among these charged particles will inevitably lead to production of photons with mean free path much larger than the size of the system formed in such collisions. As a result photons can bring the information of the state of the production point very efficiently without getting infected by the secondary interactions and therefore, considered as one of the efficient probes for the detection of QGP [1]. This has led to huge theoretical [2–12] and experimental efforts to study the mechanism of photon production in heavy ion collisions at relativistic energies (HICRE). Recent data from PHENIX [13] and ALICE [14] Collaborations at the RHIC and LHC respectively have reported excess of direct photon yield over the scaled proton-proton results in the region of transverse momentum domain, $p_T < 4$ GeV. This excess is attributed to the thermal radiation from QGP and hadronic phases. However, in spite of a large number of detailed studies by several authors [15–19] a simultaneous explanation of the data on the p_T spectra and differential elliptic flow, v_2 of photon is still lacking both for PHENIX [20] and ALICE [21] data, this has been dubbed as “direct photon puzzle” [22].

It is expected that at RHIC and LHC collision energies QGP will be formed which will evolve in space and time

and reverts to hadrons at a transition temperature, T_c . In such a scenario photons will be produced through various processes at different stages of the evolution populating different domains of p_T . These are broadly categorized as: (i) prompt photons originating from the interactions of the partons of the colliding nuclei which will populate the high p_T domain; (ii) thermal productions - from the interactions of thermal partons as well as from thermal hadrons - will occupy low and intermediate p_T and finally (iii) from the decays of the long lived (compared to strong interaction time scale) mesons. Photons from (i) are non-thermal therefore, are not affected neither by the temperature nor by the flow. Therefore, for given collision energy this contribution should be subtracted out from the data by using pQCD results. Photon spectra from proton+proton collision may be used as a benchmark to validate theoretical results. Photons from the decays of hadrons have been subtracted out from the data presented by ALICE [14] and PHENIX [13] Collaborations. Photons from thermal source, (ii) are sensitive to temperature and flow, therefore, this is the component of the spectra that needs urgent attention to address the “direct photon puzzle”.

Elliptic flow is considered as one of the fundamental observable of collectivity of the system produced in HICRE. It is well known that the v_2 of direct photon is dominated by thermal radiation and contributions from all other non-thermal sources are almost negligible. Thermal photons originating from expanding QGP along with prompt photons explain the data on the photon spectra both for Au+Au collisions at RHIC and for Pb+Pb collisions at the LHC energies in the region $p_T > 2$ GeV [23, 24]. However, the large discrepancies between theoretical results and the data on thermal photon’s v_2 remains a puzzle. Several studies such as calculations based on sophisticated event-by-event viscous hydrodynamic model as well as studies incorporating pre-equilibrium contributions, inclusion of the effects of high initial magnetic field are unable to explain the data on v_2 of photons till date.

With the increase in the precision of experimental mea-

*Electronic address: pingaldg@vecc.gov.in

†Electronic address: rupa@vecc.gov.in

‡Electronic address: sushantsk@vecc.gov.in

§Electronic address: jane@vecc.gov.in

surements it becomes imperative for theoretical calculations to include finer physical effects. One such effect is shadowing of nucleons deep inside the colliding nuclei by the nucleons at the front during the process of collisions. In an effort to understand the correlation between the multiplicity and eccentricity, effect of shadowing was included in [25, 26] in the Monte-Carlo Glauber model to deduce the initial energy density profile required as an input to the relativistic hydrodynamical equations used to understand the development of collectivity in the system. It was observed that the inclusion of shadowing in the Monte-Carlo (MC) Glauber model increases the elliptic flow significantly compared to the result obtained from the conventional MC Glauber initial condition. In this paper, we explore the effects of nucleon shadowing on the elliptic flow of photons at RHIC and LHC energies.

The paper is organized as follows. In the next section we will discuss the MC Glauber model with and without shadowing effects. Production mechanisms of photons from QGP and HM have been briefly discussed in section III with appropriate references for details. The effects of shadowing on the hydrodynamic evolution and elliptic flow of thermal photon spectra have been presented in section IV. Section V is devoted to summary and conclusions.

II. INITIAL CONDITIONS

In the conventional Monte Carlo (MC) Glauber model, all the nucleons participating in the collision process are treated democratically i.e. they receive same weightage for energy deposition through the entire collision processes. In Ref. [25] it is argued that the nucleons located deep inside the nucleus are eclipsed or shadowed by the nucleons in the front. Therefore, the contribution of a participating nucleon to energy deposition will crucially depend on its position in the colliding nuclei. This is accomplished by introducing a suppression factor $S(n, \lambda)$ in the initial state as follows:

$$S(n, \lambda) = \exp(-n\lambda) \quad (1)$$

where $S(n, \lambda)$ accounts for the shadowing on a participant due to n other nucleons in the same nucleus which are in front and conceal it partially (see Refs. [25, 26] for more detail). For the present work we consider the value of $\lambda = 0.12$ at RHIC and $\lambda = 0.08$ at LHC [25, 26]. We call the MC Glauber initial condition without the nucleon shadowing effect as MCG and the initial condition with the shadowing as shMCG.

A MC Glauber model with standard two-parameter Woods-Saxon nuclear density profile is used to randomly distribute the nucleons into the two colliding nuclei. Two nucleons from different nuclei are assumed to collide when the relation $d^2 < \frac{\sigma_{NN}}{\pi}$ is satisfied where, d is the transverse distance between the colliding nucleons and σ_{NN} is the inelastic nucleon nucleon cross-section. We

take σ_{NN} as 42 mb and 64 mb for 200A GeV Au+Au collision at RHIC and 2.76A TeV Pb+Pb collision at LHC respectively.

For the collision of two nuclei, we assume the beam axis to be along z -direction and impact parameter to be along x -direction for a particular event. The plane spanned by the x -axis and y -axis is the transverse plane. The initial entropy distribution in the transverse plane is taken as proportional to a linear combination of number of participant n_{part} and number of binary collisions n_{coll} ,

$$s(x, y) \propto \nu n_{\text{coll}}(x, y) + (1 - \nu) n_{\text{part}}(x, y) \quad (2)$$

The sensitivity of the results on ν will be studied by calculating p_T spectra and elliptic flow of photons with $\nu=0$ (wounded nucleon profile only) as well as $\nu \neq 0$ (inclusion of multiple scattering). A Gaussian distribution function of the form:

$$s(x, y) = \frac{K}{2\pi\sigma^2} \sum_{i=1}^{N_{\text{part}}, N_{\text{coll}}} \exp\left(-\frac{(x-x_i)^2 + (y-y_i)^2}{2\sigma^2}\right) \quad (3)$$

is used to distribute the initial entropy density. K in Eq. 3 is a constant (fixed from experimental charged particle multiplicity) and the position of the i th nucleon in the transverse plane is denoted by (x_i, y_i) . σ is a free parameter, taken as $\sigma = 0.4$ fm [23, 27] in this work. We take the values of initial thermalization times for RHIC and LHC as $\tau_0 = 0.17$ fm/c and 0.14 fm/c respectively from the EKRT mini-jet saturation model [28].

In the present work, a (2+1) dimensional inviscid relativistic hydrodynamic model has been used to study the space-time evolution of the matter produced in HI-CRE [27]. This hydrodynamic framework with MCG initial conditions has been used earlier to study spectra and anisotropic flow of hadrons and photons [23, 24, 27]. We modify the initial conditions to include the shadowing effect.

The initial entropy density profile required as input to hydrodynamical calculation is constructed for both the cases (MCG and shMCG) by taking initial state average of 10000 random events. The equation of state (EoS) [29] has been taken from lattice QCD calculations. The freeze-out condition is constrained by the p_T spectra of charged pions.

III. PHOTONS FROM THERMAL QGP AND HADRONS

Contributions from the QGP phase to the thermal spectra due to annihilation ($q\bar{q} \rightarrow g\gamma$) and the QCD Compton ($q(\bar{q})g \rightarrow q(\bar{q})\gamma$) processes to the order $\alpha_s\alpha$ was estimated in [30, 31] by using hard thermal loop (HTL) approximation [32]. Later, it was shown that photons from the processes [33]: $gq \rightarrow gq\gamma$, $qq \rightarrow qq\gamma$, $qq\bar{q} \rightarrow q\gamma$ and $gq\bar{q} \rightarrow g\gamma$ contribute also to the same order as $O(\alpha\alpha_s)$. The complete calculation of emission rate from QGP to

order α_s has been performed by resumming ladder diagrams in the effective theory [34, 35]. In the present work the rate of production of thermal photon has been taken from [34]. The T dependence of the strong coupling, α_s has been taken from [36].

For the photon production from hadronic phase an exhaustive set of hadronic reactions and the radiative decay of higher resonance states are considered. The rate has been taken from [37] which includes the effects of the hadronic form factor (see also [38–40]).

The p_T distribution of photons that can be contrasted with data is obtained by integrating the emission rates ($R = EdN/d^3pd^4x$) at a fixed temperature over the entire space-time evolution history - from the initial thermalization time to the final freeze-out state of the fireball via intermediary quark-hadron phase transition as:

$$E \frac{dN}{d^3p} = \int d^4x R(E^*(x), T(x)) \quad (4)$$

where $T(x)$ is the local temperature and $E^*(x) = p^\mu u_\mu(x)$ is the energy in the comoving frame, p^μ is the four-momentum of the photons and u_μ is the local four-velocity of the flow field. T and u^μ are obtained from the solution of hydrodynamical equations.

The elliptic flow parameter v_2 can be calculated using the relation:

$$v_2(p_T) = \langle \cos(2\phi) \rangle = \frac{\int_0^{2\pi} d\phi \cos(2\phi) \frac{dN}{p_T dp_T dy d\phi}}{\int_0^{2\pi} d\phi \frac{dN}{p_T dp_T dy d\phi}} \quad (5)$$

The temperature at freeze-out is taken as 160 MeV which reproduces the measured p_T spectra of charged pions at RHIC and LHC energies. The value of quark-hadron transition temperature is taken as 170 MeV and the lattice QCD based EoS is taken from [29].

IV. RESULTS

As discussed above we consider the following scenarios in presenting the results. The space-time evolution of the fireball has been considered with and without shadowing by taking (a) $\nu = 0$ and (b) $\nu \neq 0$ in Eq. 2, where ν is constrained to reproduce the charged multiplicity observed in experiments.

(a) First we consider a wounded nucleon profile ($\nu = 0$) and study the evolution of the hot and dense system with two kinds of initial energy density profiles resulting from the inclusion and exclusion of shadowing effects. The averages are calculated using the relation

$$\langle f \rangle = \frac{\int dx dy f(x, y) \epsilon(x, y, \tau)}{\int dx dy \epsilon(x, y, \tau)} \quad (6)$$

where $\epsilon(x, y, \tau)$ is the energy density obtained by solving the hydrodynamic equations. The time evolution of average temperature, $\langle T \rangle$ (upper panel) and average transverse flow velocity, $\langle v_T \rangle$ (lower panel) for MCG and

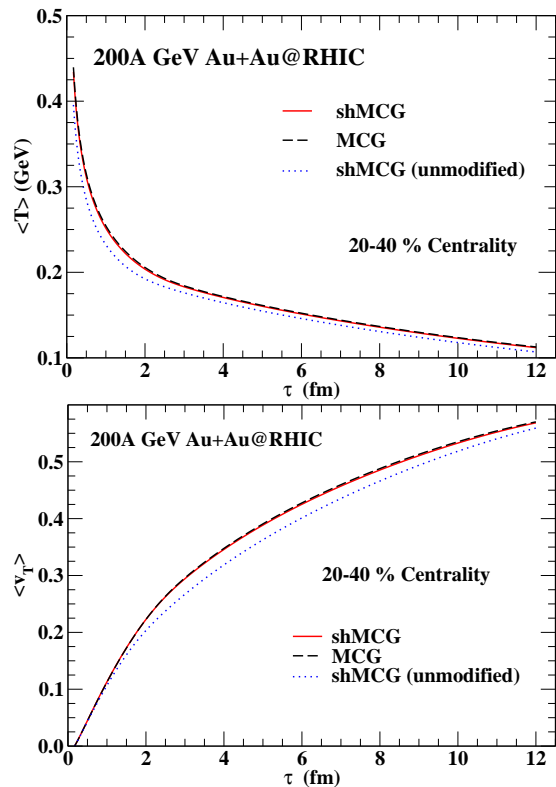


FIG. 1: (Color online) Time evolution of average temperature and transverse flow velocity with MCG and shMCG initial conditions have been depicted for $\nu = 0$.

shMCG initial conditions for 200A GeV Au+Au collisions at RHIC in 20 – 40% centrality bin are shown in Fig. 1. We take $K = 102 \text{ fm}^{-1}$ for MCG initial condition.

The time evolution of $\langle T \rangle$ and $\langle v_T \rangle$ have been estimated by considering an entropy initialized wounded nucleon profile in ideal hydrodynamic model calculation and smooth initial entropy density distribution.

The MCG initial condition has been used extensively earlier to calculate photon production at RHIC and at the LHC energies [23, 24]. The inclusion of initial state shadowing, *i.e.* $\lambda \neq 0$, in the MCG initial condition and without changing any other parameter (from now on we call this as unmodified shMCG) results in smaller charged multiplicity or total entropy, which will obviously lead to smaller average temperature and pressure. This will lead to smaller average transverse flow velocity too (shown by blue dotted lines).

In order to obtain the initial condition for shMCG, the normalization factor K in Eq. 3 is tuned to reproduce the same final $dN_{\text{ch}}/d\eta$ as MCG initial condition. We obtain $K = 140 \text{ fm}^{-1}$ for shMCG. The time evolution of $\langle T \rangle$ and $\langle v_T \rangle$ in the MCG and shMCG scenarios are found to be close to each other as shown by black dashed and red solid lines respectively.

Next we display our results on the p_T spectra of photon. The upper panel of Fig. 2 shows the thermal photon

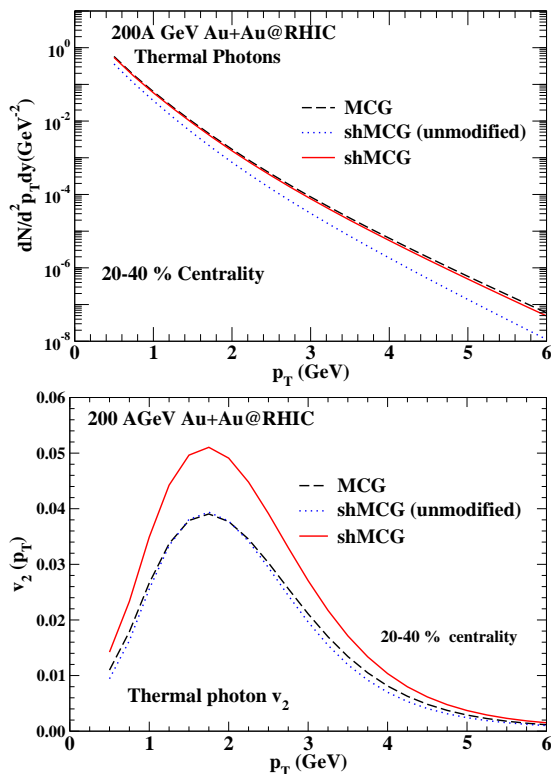


FIG. 2: (Color online) Thermal photon spectra and elliptic flow from MCG and shMCG initial conditions for wounded profile at RHIC 200A GeV Au+Au collisions in 20–40% centrality bin.

spectra with MCG and shMCG initial conditions for 20–40% central Au+Au collisions at RHIC. For given production rate of photons and with similar space-time evolution scenario the spectra for the two initial conditions (MCG and shMCG) are found to be close to each other. For both the cases, photon spectra are dominated by radiation from the QGP phase for $p_T > 1$ GeV and only in the low p_T (< 1 GeV) region we see significant contribution from the hadronic phase.

The elliptic flow of thermal photons calculated using MCG and shMCG initial conditions are shown in the lower panel of Fig. 2. As shown in earlier studies [24, 41], due to the competing contributions from the quark matter and hadronic matter (HM) phases, the v_2 of photons shows different nature compared to that of hadrons. Because photons are emitted from every space-time point and hence is able to trace the entire history of evolution - from the early stage of maximal asymmetry and minimal flow - to the late stage of reduced asymmetry and larger flow. In contrast to photons, hadrons are predominantly emitted from the late freeze-out stage of the evolution. The differential elliptic flow of photon is small at large p_T as these are mostly emitted from the (early) QGP phase where the flow has not developed fully. As we approach from high p_T , the $v_2(p_T)$ increases towards smaller values of p_T , reaches maximum around 1.5 - 2.0 GeV and

then drops as p_T is reduced further. Such a variation of $v_2(p_T)$ results from the two competing profiles of elliptic flow originating from QGP and hadronic phases (see later).

We see a significant increase in the elliptic flow for the shMCG initial condition compared to the MCG initial condition. The value of $v_2(p_T)$ at the peak is about 32% larger in the shMCG case. The inclusion of shadowing in the initial condition affects the nucleons at the interior more than those at the boundary [25]. Hence, the effects of shadowing at the end of the major axis is smaller than at the end of the minor axis of the ellipsoidal shaped overlapped zone. Because at the end of the major axis the nucleons from the boundary of the two nuclei are involved where the effects of shadowing is minimal. In contrast at the end of the minor axis, nucleons from the interior of one of the nuclei with large shadowing effects collide with the nucleons from the boundary of the other nucleus. Therefore, the effective length of the minor axis is smaller in shMCG than MCG. As a consequence the pressure gradient in shMCG is larger resulting in larger elliptic flow. Interestingly, one can see that the v_2 from the unmodified shMCG initial condition, in which shadowing is included but K is not fixed to reproduce the final particle multiplicity, is close to the v_2 from MCG initial condition even when shadowing introduces more spatial anisotropy. This is because of the lower pressure in case of unmodified shMCG scenario (Fig. 1).

In the present study we consider initial state averaged smooth density distribution only and show that even though the photon spectra remain unaltered, the effect of shadowing on the elliptic flow is significantly large. It has been shown earlier that elliptic flow from event-by-event fluctuating initial conditions increases v_2 significantly in the region $p_T > 2$ GeV compared to the v_2 calculated from a smooth initial state averaged profile [4]. Thus, result from calculation based on event-by-event fluctuating initial condition with the inclusion of shadowing effect is expected to enhance the v_2 . This would reduce the difference between the experimental data and theoretical results and would help in resolving the existing “direct photon puzzle”. In addition, photon v_3 which originates from the initial state fluctuations only, is also expected to be larger using shMCG initial condition. We postpone these for a future study [42].

(b) Next we consider the case, $\nu \neq 0$. The nucleon shadowing is expected to affect N_{coll} more strongly than N_{part} . Therefore, we consider Au+Au collisions at RHIC where the initial entropy density is taken as proportional to a linear combination of N_{coll} and N_{part} . We take $\nu = 0.14$, $K = 80 \text{ fm}^{-1}$ for the MCG initial state and $\nu = 0.31$ and $K = 110 \text{ fm}^{-1}$ for shMCG. The p_T spectra of π^+ has been evaluated including the feed-down from higher resonance decays at the freeze-out surface by using Cooper -Frye [43] formula. The result has been contrasted with experimental data from RHIC [44]. We find that the spectra for MCG and shMCG are similar and both are close to experimental data (Fig.4).

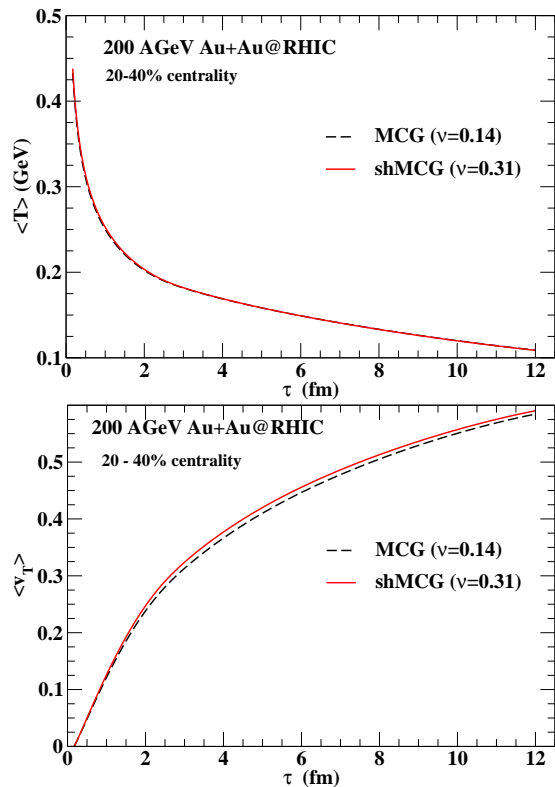


FIG. 3: (Color online) Time evolution of average transverse flow velocity and average temperature considering MCG and shMCG initial states for two component model.

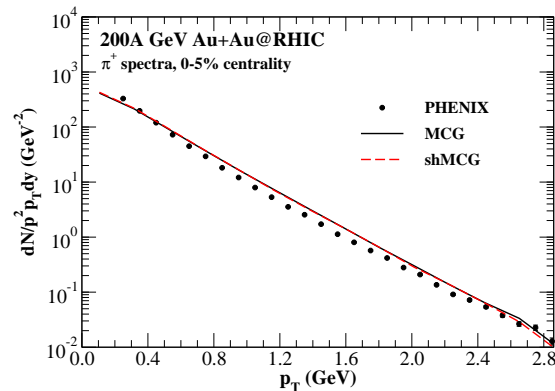


FIG. 4: (Color online) The thermal pion spectra at RHIC with two types of initial condition (see text) and comparison with PHENIX data [44].

The time evolution of $\langle T \rangle$ and $\langle v_T \rangle$ for two initial conditions (MCG and shMCG) are shown in Fig. 3. The $\langle T \rangle$ for both the cases are almost on top of each other whereas, the $\langle v_T \rangle$ is found to be marginally larger for shMCG initial condition. For $\nu \neq 0$ a nucleon undergo several collisions unlike the case for $\nu = 0$ where a nucleon undergo single collision. For mid-central collisions, a different amount of energy is deposited in successive binary collisions for $\nu \neq 0$ which results in large shadowing ef-

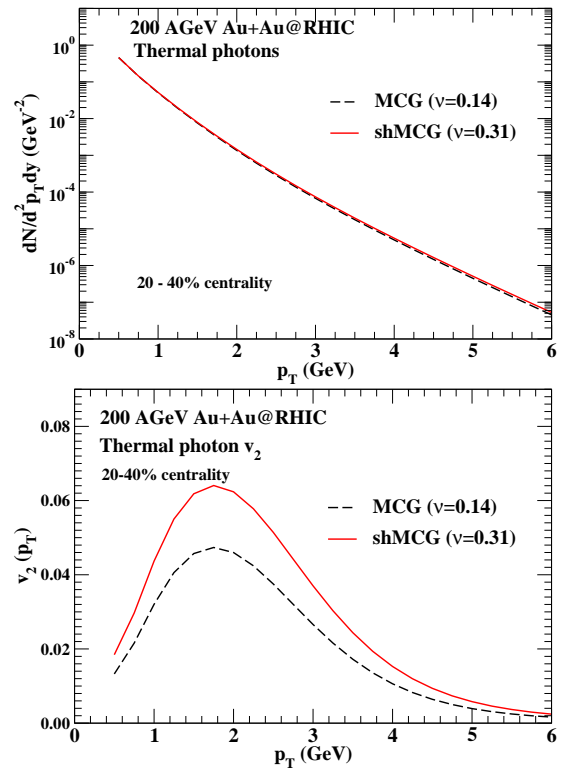


FIG. 5: (Color online) Thermal photon spectra and elliptic flow considering MCG and shMCG initial conditions for 200A GeV Au+Au collisions at RHIC and 20–40% centrality bin for two component model.

fects compared to wounded nucleon initial condition. As a consequence the pressure gradient in shMCG is larger resulting in slightly larger transverse flow as shown in Fig. 3.

The corresponding spectra and elliptic flow of thermal photons are shown in Fig. 5. The nature of the p_T spectra and elliptic flow is found to be similar to the results from wounded nucleon profile. As shown in the figure, the p_T spectra using the MCG and shMCG initial conditions are again found to be very close to each other. However, the elliptic flow is found to be slightly larger for two component initial conditions compared to the v_2 from corresponding single component ($\nu = 0$) model. In addition, peak value of $v_2(p_T)$ for shMCG initial condition is found to be about 36% larger than the $v_2(p_T)$ calculated using the MCG initial condition. Moreover, as mentioned above the effects of shadowing at the end of the major axis is smaller than at the end of the minor axis of ellipsoidal shaped overlapped zone, which effectively reduces the minor to major axis ratio in shMCG compared to MCG resulting in larger elliptic flow in the shMCG scenario.

In order to understand the effect of initial state shadowing on the photon elliptic flow better, we plot the spectra and elliptic flow from individual QGP and HM phases separately in Fig. 6. The thermal photon spectra as expected both from QGP and HM phases are close to each

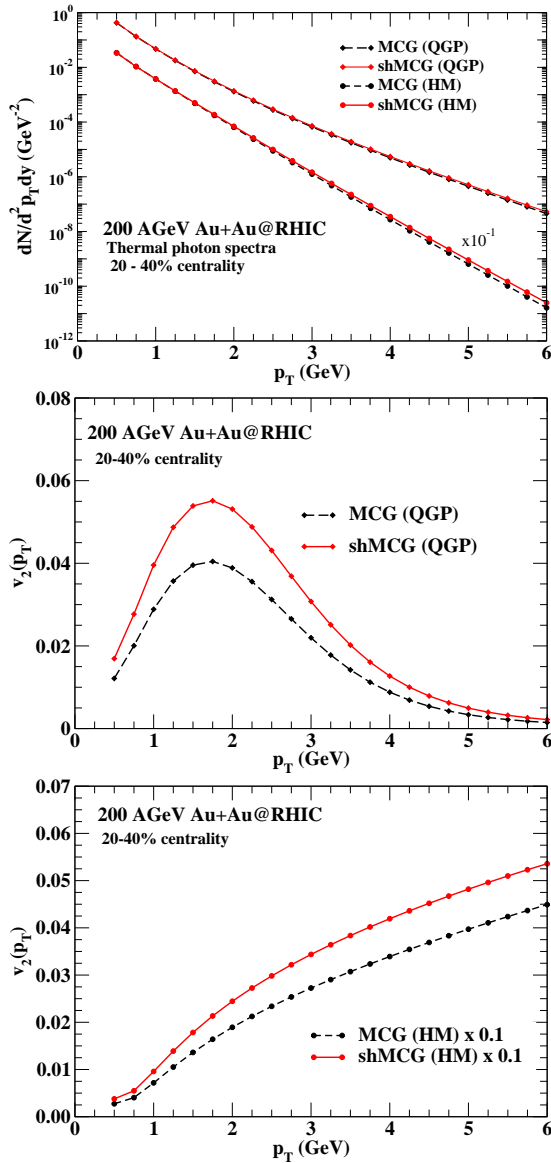


FIG. 6: (Color online) Thermal photon spectra and elliptic flow from QGP and HM phases separately from MCG and shMCG initial conditions.

other for the two different initial conditions. The effect of initial state shadowing is found to be more pronounced for v_2 of photon from QGP compared to v_2 from HM phase. The maximum value of $v_2(p_T)$ is about 50% larger for shMCG initial state compared to the MCG initial state in the QGP phase. A similar trend is observed in the v_2 of photons from hadronic matter. The net v_2 from the entire space-time evolution has been shown earlier in Fig. 5.

Next we consider Pb+Pb collision at 2.76A TeV energy at the LHC. We evaluate the p_T spectra of thermal photon and elliptic flow using MCG and shMCG initial conditions.

We take $\nu = 0.11$, $K = 192 \text{ fm}^{-1}$ for the MCG initial state and $\nu = 0.32$, $K = 223 \text{ fm}^{-1}$ for the shMCG

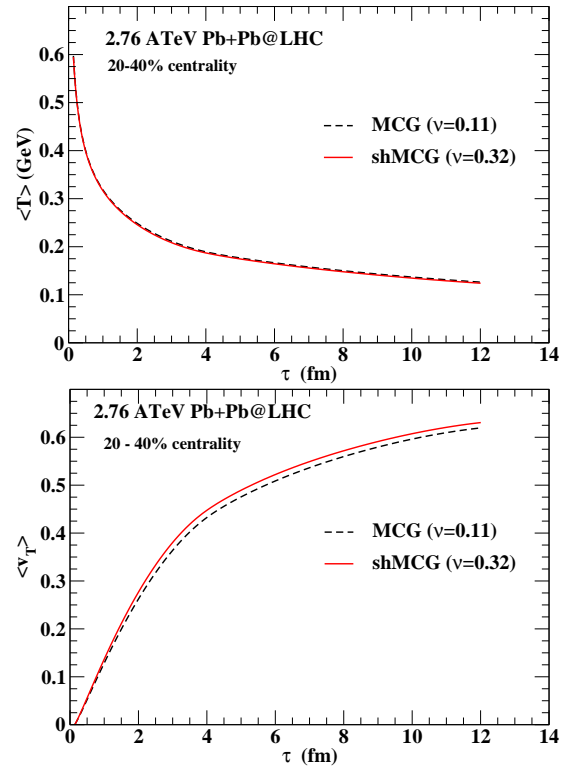


FIG. 7: (Color online) The time evolution of temperature and transverse velocity estimated for LHC energy with two types of initial conditions (see text).

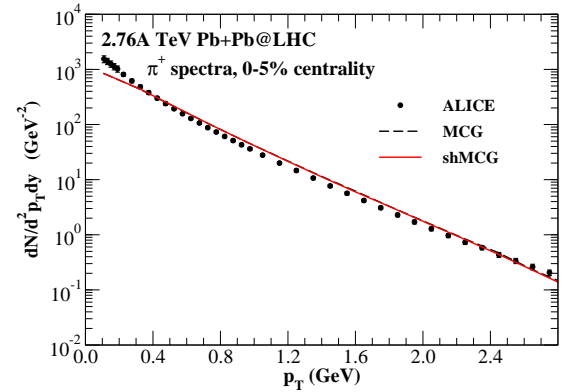


FIG. 8: (Color online) The thermal pion spectra evaluated for LHC with two types of initial conditions (see text) and comparison with ALICE data [45].

initial condition. In Fig. 7 we display the variation of average temperature and transverse velocity with τ for LHC energy. Although, the result is qualitatively similar to RHIC, however, quantitatively the values of $\langle T \rangle$ and $\langle v_T \rangle$ are larger at LHC because of the larger initial temperature and pressure.

The π^+ spectra for LHC collision condition has been evaluated at the freeze-out surface and the results are compared with the experimental data [45]. The spectra

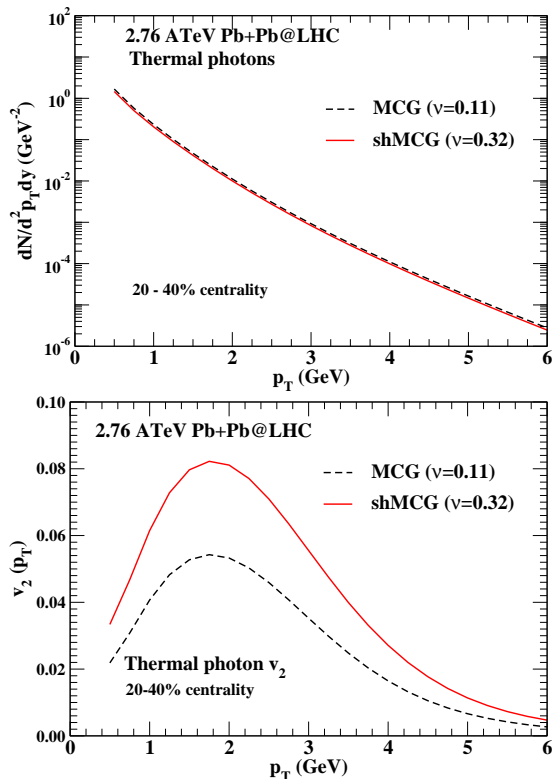


FIG. 9: (Color online) The p_T spectra and v_2 of thermal photon for LHC energy with two types of initial conditions (see text).

from MCG and shMCG are similar (Fig. 8).

Finally in Fig. 9 the transverse momentum spectra of photon and v_2 of photon has been depicted for LHC collision condition. The effects of shadowing does not show up in the p_T spectra of photons (upper panel). However, the elliptic flow gets about 50% enhanced at peak value in shMCG as compared to MCG for reasons explained earlier.

V. SUMMARY AND CONCLUSIONS

We have considered the effect of nucleon shadowing in the MC Glauber initial condition and calculate thermal

photon spectra and elliptic flow for 200A GeV Au+Au collision at RHIC and 2.76A TeV Pb+Pb collision at LHC for 20 – 40% centrality. The initial conditions both for MCG and shMCG are constrained to the same charged multiplicity for RHIC as well as LHC collision conditions. Results without this constraints have also been shown. (2+1) dimensional relativistic hydrodynamic equations has been solved with lattice QCD EoS to study the space time evolution of the system. We calculate photon spectra and elliptic flow considering both wounded nucleon as well as a two component model where the initial energy is taken to be proportional to a linear combination of N_{coll} and N_{part} . The results on the p_T spectra of photons and pions both from RHIC and LHC collision conditions are found to be insensitive to the shadowing effects if the initial conditions are restrained to reproduce the same charged multiplicity. However, with the same situation the elliptic flow from shMCG initial condition is found to be significantly larger compared to the MCG initial condition. As discussed in the text the shadowing enhances the asymmetry by decreasing the effective ratio of minor to major axis of the ellipsoidal shaped reaction zone. Therefore, the shadowing effects has the potential to affect those quantities which depends on the geometric asymmetry of the system formed in HICRE. By taking initial state average of random events the contribution from the initial state fluctuations to v_2 has been discounted here. Therefore, a complete calculation considering initial state shadowing for an event-by-event fluctuating initial condition would be very useful to understand the v_2 of photons originating from QGP and hot hadrons. Because it will contain contributions to v_2 both from the initial fluctuations as well as non-spherical geometry of the collision zone.

VI. ACKNOWLEDGEMENTS

We thank C&I group, VECC for providing computer facility and PDG is grateful to Department of Atomic Energy for financial support. Discussions with Dinesh Kumar Srivastava and Snigdha Ghosh are gratefully acknowledged.

-
- [1] J. Alam, B. Sinha, S. Raha, Phys. Rep. **273**, 243 (1996)
 - [2] D. K. Srivastava, J. Phys. G **35**, 104026 (2008).
 - [3] C. Gale, Y. Hidaka, S. Jeon, S. Lin, J.-F. Paquet, R. D. Pisarski, D. Satwo, V. V. Spokov and G. Vujanovic, Phys. Rev. Lett. **114**, 072301 (2015).
 - [4] R. Chatterjee, H. Holopainen, I. Helenius, T. Renk, K. J. Eskola, Phys. Rev. C **88**, 034901 (2013).
 - [5] C. Shen, U. Heinz, J.-F. Paquet, I. Kozlov and C. Gale, Phys. Rev. C **91**, 024908 (2015).
 - [6] A. Monnai, Phys. Rev. C **90**, 021901 (2014).
 - [7] L. McLerran and B. Schenke, Nucl. Phys. A **929**, 71 (2014).
 - [8] F.-M. Liu and S.-X. Liu, Phys. Rev. C **89**, 034906 (2014).
 - [9] G. Basar, D. E. Kharzeev and V. Skokov, Phys. Rev. Lett. **109**, 202303 (2012).
 - [10] K. Tuchin, Phys. Rev. C **87**, 024912 (2013).
 - [11] B. G. Zakharov, Eur. Phys. J. C **76**, 609 (2016).
 - [12] G. Vujanovic, J. F. Paquet, G. S. Denicol, M. Luzum, B. Schenke, S. Jeon and C. Gale, Nucl. Phys. A **932**, 230

- (2014).
- [13] A. Adare *et al.* (PHENIX Collaboration) Phys. Rev. Lett. **104**, 132301 (2010), A. Adare *et al.* (PHENIX Collaboration), Phys. Rev. C **91**, 064904 (2015).
- [14] M. Wilde for the ALICE Collaboration, Nucl. Phys. A **904-905**, 573c (2013); J. Adam *et al.* (ALICE Collaboration), Phys. Lett. B **754**, 235 (2016).
- [15] S. Ryu, J. F. Paquet, C. Shen, G. S. Denicol, B. Schenke, S. Jeon and C. Gale, Phys. Rev. Lett. **115**, 132301 (2015).
- [16] J. F. Paquet, C. Shen, G. S. Denicol, M. Luzum, B. Schenke, S. Jeon and C. Gale, Phys. Rev. C **93**, 044906 (2016).
- [17] H. van Hees, M. He and R. Rapp, Nucl. Phys. A **933**, 256 (2015).
- [18] H. van Hees, C. Gale and R. Rapp, Phys. Rev. C **84**, 054906 (2011).
- [19] O. Linyuk, W. Cassing and E.L. Bratkovskaya, Phys. Rev. C **89**, 034908 (2014).
- [20] A. Adare *et al.* (PHENIX Collaboration) Phys. Rev. Lett. **109**, 122302 (2012); A. Adare *et al.* (PHENIX Collaboration) Phys. Rev. C **94**, 064901 (2016).
- [21] D. Lohner for the ALICE Collaboration, J. Phys. Conf. Ser. **446**, 012028 (2013).
- [22] <http://cerncourier.com/cws/article/cern/63155>.
- [23] R. Chatterjee, H. Holopainen, T. Renk, and K. J. Eskola, Phys. Rev. C **83**, 054908 (2011); R. Chatterjee, H. Holopainen, T. Renk, K. J. Eskola, J. Phys. G. Nucl. Part. Phys. **38**, 124136 (2011).
- [24] R. Chatterjee H. Holopainen, T. Renk, and K. J. Eskola, Phys. Rev. C **85**, 064910 (2012); R. Chatterjee H. Holopainen, T. Renk, and K. J. Eskola, arXiv:1207.6917.
- [25] S. Chatterjee, S. K. Singh, S. Ghosh, Md. Hasanujjaman, J. Alam, and S. Sarkar, Phys. Lett. B **758**, 269 (2016).
- [26] S. Ghosh, S. K. Singh, S. Chatterjee, J. Alam, and S. Sarkar, Phys. Rev. C **93**, 054904 (2016).
- [27] H. Holopainen, H. Niemi, and K. Eskola, Phys. Rev. C **83**, 034901 (2011).
- [28] K. J. Eskola, K. Kajantie, P. V. Ruuskanen, and K. Tuominen, Nucl. Phys. B **570**, 379 (2000).
- [29] M. Laine and Y. Schroder, Phys. Rev. D **73**, 085009 (2006).
- [30] J. Kapusta, P. Lichard, and D. Seibert, Phys. Rev. D **44**, 2774 (1991).
- [31] R. Bair, H. Nakkagawa, A. Niegawa, and K. Redlich, Z. Phys. C **53**, 433 (1992).
- [32] E. Braaten and R. D. Pisarski, Nucl. Phys. B **337**, 569 (1990); *ibid* **339**, 310 (1990).
- [33] P. Aurenche, F. Gelis, R. Kobes, and H. Zaraket, Phys. Rev. D **58**, 085003 (1998).
- [34] P. Arnold, G. D. Moore, and L.G. Yaffe, J. High Energy Phys. **0111**, 057 (2001) ; P. Arnold, G.D. Moore, and L.G. Yaffe, J. High Energy Phys. **0112**, 009 (2001) ; P. Arnold, G.D. Moore, and L.G. Yaffe, J. High Energy Phys. **0206**, 030 (2002).
- [35] J. Ghiglieri, J. Hong, A. Kurkela, E. Lu, G. D. Moore, and D. Teaney, JHEP **1305**, 010 (2013).
- [36] O. Kaczmarek and F. Zantow Phys. Rev. D **71**, 114510 (2005).
- [37] S. Turbide, R. Rapp, and C. Gale, Phys. Rev. C **69**, 014903 (2004).
- [38] S. Sarkar, J. Alam, P. Roy, A. K. Dutt-Mazumder, B. Dutta-Roy and B. Sinha, Nucl. Phys. A **634**, 206 (1998).
- [39] P. Roy, S. Sarkar, J. Alam and B. Sinha, Nucl. Phys. A **653**, 277 (1999).
- [40] J. Alam, P. Roy and S. Sarkar Phys. Rev. C **71**, 059802 (2005).
- [41] R. Chatterjee, E. Frodermann, U. W. Heinz, and D. K. Srivastava, Phys. Rev. Lett. **96**, 202302 (2006); R. Chatterjee and D. K. Srivastava, Phys. Rev. C **79**, 021901(R) (2009); U. W. Heinz, R. Chatterjee, E. S. Frodermann, C. Gale, and D. K. Srivastava, Nucl. Phys. A **783**, 379 (2007).
- [42] P. Dasgupta *et al.* [in preparation].
- [43] F. Cooper and G. Frye, Phys. Rev. D **10**, 186 (1974).
- [44] S. S. Adler *et al.*, Phys. Rev. C **69**, 034909 (2004).
- [45] B. Abelev *et al.*, Phys. Rev. C **88**, 044910 (2013).